Diffusion-free image storage in hot atomic vapor

Young-Wook Cho,* Joo-Eon Oh, and Yoon-Ho Kim†
Department of Physics, Pohang University of Science and Technology (POSTECH), Pohang 790-784, Korea
(Received 22 March 2012; published 30 July 2012)

The ability to directly store optical images in atomic vapor has many potential applications, but the diffusion of atoms severely limits the image resolution and storage duration. In this paper, we report an experimental demonstration on diffusion-free storage of optical images in hot atomic vapor. By encoding two-dimensional images in incoherent light and making use of the correlation imaging technique, we overcome the effect of atomic diffusion on the all-optical image storage in atomic vapor.

DOI: 10.1103/PhysRevA.86.013844 PACS number(s): 42.50.Gy, 32.80.Qk, 42.30.−d, 42.50.Ar

The slow light and light storage technologies have attracted significant interest in recent years [1–5] and are expected to play important roles in both classical and quantum information systems, e.g., all-optical buffers and routers, quantum memories, etc. [6,7]. Lately, the technology has been expanded to buffering and storing two-dimensional optical information (i.e., optical images): All-optical image delay has been demonstrated using atomic vapor [8] and using cavity resonance [9,10]. Also, coherent storage of optical images has been demonstrated by utilizing electromagnetically induced transparency (EIT) in atomic vapor [11–14] and in a crystal at a cryogenic temperature [15].

For image storage in a crystal, not only is a specialized crystal (Pr:YSO in Ref. [15]) required, but it also must be cooled down to temperatures below 4 K, making the scheme less practical. A more practical and functional scheme would be to use warm (or hot) atomic vapor for storing optical images, but atomic diffusion puts a severe restriction on the quality of the retrieved images. There exist ways to reduce the effect of atomic diffusion on the quality of retrieved images either by using the optical phase-shift lithography technique [11,12] or by storing the Fourier transform of the image (i.e., the diffraction pattern) rather than storing the image directly [13,14].

Since both of these methods are based on the destructive interference originating from the transverse spatial coherence of the dark-state polariton [16], they are not applicable to remove the effect of atomic diffusion on the retrieved image if the optical image is produced with incoherent light. Furthermore, these approaches, based on destructive interference, have serious drawbacks for practical image storage. In the case of optical phase-shift lithography, it is necessary to prepare a specific phase plate for each image, thus, rending the approach impractical for storing arbitrary images. For the Fourier-transform storage method, it is necessary that the length of the atomic vapor cell is much shorter than the focal length of the Fourier-transform lens. A short atomic vapor cell offers very limited storage duration because of the small optical depth. It should also be mentioned that the Fourier-transform storage method is valid only for a simple binary object and does not work for a continuous varying grayscale image [14].

In this paper, we demonstrate diffusion-free optical image storage in warm atomic vapor with incoherent light. The two-dimensional optical image is carried by incoherent (i.e., thermal) light and, by making use of the ghost imaging or the correlation imaging technique [17–20], we demonstrate that it is possible to completely remove the effect of atomic diffusion for two-dimensional optical image storage in atomic vapor.

Let us begin by describing the experimental setup schematically shown in Fig. 1. An incoherent light beam, having the thermal (i.e., Bose-Einstein) photon statistics, is generated by focusing a laser beam at a rotating ground disk. The laser beam is frequency stabilized at the ^{87}Rb D_1 line ($|F=2\rangle \rightarrow |F'=2\rangle$), and the generated incoherent light beam has a sufficiently narrow bandwidth to coherently interact with the atom [21]. The temporal second-order correlation function $g^{(2)}(\tau)$, measured with the Hanbury-Brown–Twiss interferometer, exhibits the characteristic photon-bunching effect in the time domain with $g^{(2)}(\tau) = 1 + \exp[-\pi(\tau/\tau_c)^2]$, where the coherence time $\tau_c = 7.26 \pm 0.07$ μs. The incoherent light beam also exhibits the transverse spatial photon-bunching effect. The spatial intensity autocorrelation function measured with a CCD with the effective gating time of 4 μs gives $g^{(2)}(x - x' = 0) = 1.6$, which is smaller than the ideal value of 2. This discrepancy is due to the fact that the CCD, even with a short effective window, accepts substantial background noise. The transverse spatial second-order correlation function is measured to be $g^{(2)}(x - x') = 1 + 0.6 \exp[-\pi(x - x')^2/x_c^2]$ with the coherence radius $x_c = 92.8$ μm, which determines the resolution of the correlation imaging or the ghost imaging technique. Note that the coherence radius x_c can be reduced significantly for high-resolution correlation imaging [17,18].

The incoherent light beam is then split into two spatially correlated twin beams by using a polarizing beam splitter (PBS1). The horizontally polarized transmitted beam (reference beam) is captured by a CCD camera. The vertically polarized reflected beam (signal beam) illuminates an object mask (USAF-1951 resolution target, Newport RES-1), and the light transmitted through the mask is collected into a multimode optical fiber so that any direct imaging information is erased. The signal beam, after passing through the multimode fiber, is then collimated and is polarization filtered with a horizontal polarizer (Pol) for efficient storage in ^{87}Rb atomic vapor. The signal beam and the vertically polarized coupling

*choyoungwook81@gmail.com
†yoonho72@gmail.com

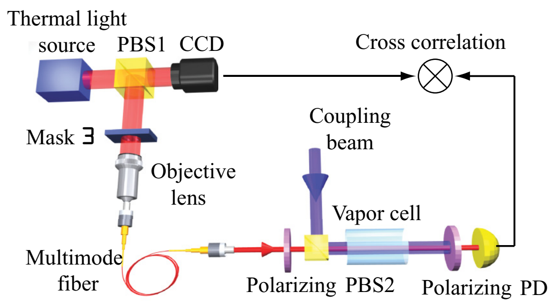

FIG. 1. (Color online) Schematic of the experimental setup. An incoherent light beam is split into two with a polarizing beam splitter (PBS1). The reflected beam passes through the mask, is collected and is collimated with a multimode fiber, and gets stored in the atomic vapor using the EIT effect. The retrieved beam is then detected with a photodiode (PD) with no spatial resolution. The transmitted beam, which has no information about the mask, is imaged with a CCD camera. The image of the mask is reconstructed by correlating the outputs of PD and CCD which, individually, carry no information about the mask.

beam are then made to overlap spatially at the polarizing beam splitter (PBS2) and are directed to the EIT medium, which is a 75-mm long anti-reflection-coated ^{87}Rb vapor cell with 10-Torr Ne buffer gas. The coupling laser beam is frequency locked to the ^{87}Rb D_1 line $|F=1\rangle \rightarrow |F'=2\rangle$. The coupling laser beam and the signal beam, which has incoherent thermal photon statistics, form the Λ-type EIT system for the ^{87}Rb. The vapor cell was maintained at 55 °C, providing the number density of $\sim 2\times 10^{11}$ cm^{-3}. The powers of the signal beam and the coupling beam right before the vapor cell were 50 μW and 4.5 mW, respectively. The EIT resonance bandwidth was measured to be 160 kHz at this condition, and this is wider than the linewidth of the signal beam, which is approximately 138 kHz so that the linewidth of the signal beam fits into the EIT linewidth. Finally, the vertically polarized coupling laser is filtered out with a horizontal Pol, and only the retrieved signal beam reaches the PD. Note that both the CCD and the PD have no direct imaging information about the mask: The image of the mask is reconstructed by performing the cross-correlation measurement between the outputs from the CCD and PD.

The timing sequence for the image storage and retrieval experiment is shown in Fig. 2. The signal beam and the reference beam are shaped to a 10-μs rectangular pulse by using an acousto-optic modulator [(AOM); not shown in Fig. 1]. The reference beam is captured with the CCD synchronized with the AOM. The CCD is triggered after the signal beam is turned on to reduce the effective CCD exposure time down to 4 μs. To store the signal pulse, the EIT medium is prepared by turning on the coupling laser. Once the signal pulse completely enters the vapor cell (at $t=0$), the coupling beam is immediately turned off so that the signal pulse is stored into the EIT medium. After some storage time t_s, the signal pulse is partially retrieved by temporally turning on the coupling laser for 4 μs.

As mentioned before, neither the outputs from the CCD nor the PD have information regarding the object image individually. However, by performing the cross correlation between the outputs, we are able to obtain the image of the mask. Let us denote the ith detected outputs from the PD and CCD as $I_i(t)$ and $J_i(\vec{\rho},t)$, respectively. Here, $\vec{\rho}$ refer to the transverse position at the CCD. The measurement times for both the PD and the CCD are set at 4 μs, so we have $\mathcal{I}_i(t) = \int_t^{t+4\mu s} dt' I_i(t')$ and $\mathcal{J}_i(\vec{\rho},t) = \int_t^{t+4\mu s} dt' J_i(\vec{\rho},t')$. Note that the measurement time of 4 μs is shorter than the coherence time of the signal beam to resolve the intensity fluctuation. Although each of these two values individually carries no imaging information, by performing the cross correlation of fluctuations of the two signals $\Delta\mathcal{I}_i(t) = \mathcal{I}_i(t) - \frac{1}{N}\sum_i^N \mathcal{I}_i(t)$ and $\Delta\mathcal{J}_i(\vec{\rho},t) = \mathcal{J}_i(\vec{\rho},t) - \frac{1}{N}\sum_i^N \mathcal{J}_i(\vec{\rho},t)$, where N is the total number of measurements, it is possible to extract the image. Specifically, the correlation image (or the ghost image) of the mask is obtained by using the relation $G(\vec{\rho},t_1,t_2) = \sum_i^N \Delta\mathcal{I}_i(t_1)\Delta\mathcal{J}_i(\vec{\rho},t_2)$.

Figure 3 shows the reconstructed correlation image of the mask before (0 μs) and after (4–12 μs) storage in atomic vapor. The image before storage (0 μs) corresponds to $G(\vec{\rho},t_1=-4\ \mu\text{s},\ t_2=-4\ \mu\text{s})$: A clear flipped image of the digit "3" in the OCR-A font is obtained with the total number of measurement $N=7000$. The correlation images reconstructed from the retrieved signal beams, whose storage time is t_s, correspond to $G(\vec{\rho},t_1=t_s,\ t_2=-4\ \mu\text{s})$. As before, N is set at 7000, and the data shown in Fig. 3 indicate that the image quality is hardly affected by the storage time, which varies between 4 and 12 μs.

Let us now examine what would happen with the image quality if the image had been stored directly in atomic vapor [12,13]. The experimental scheme is shown in Fig. 4(a). For image storage, a $4f$ imaging system ($f=150$ mm) is used to map the image of the mask at the center of the vapor cell. The retrieved image is then relayed to the CCD with a $2f$ imaging lens. For immediate comparison with the above result, the same vapor cell at the same temperature was used. For direct

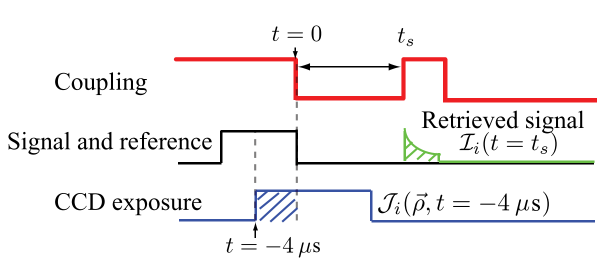

FIG. 2. (Color online) The timing sequence of the experiment. By using delayed triggering of the CCD, we achieve an effective exposure time of 4 μs for the CCD, and this helps to reduce the background noise.

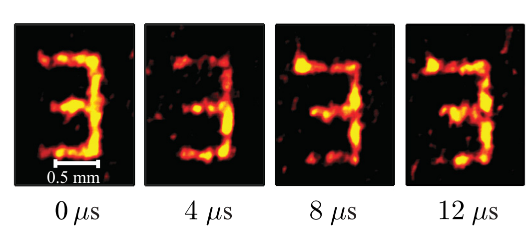

FIG. 3. (Color online) Correlation images of the mask before (0 μs) and after (4–12 μs) the storage. The retrieved images exhibit no diffusion.

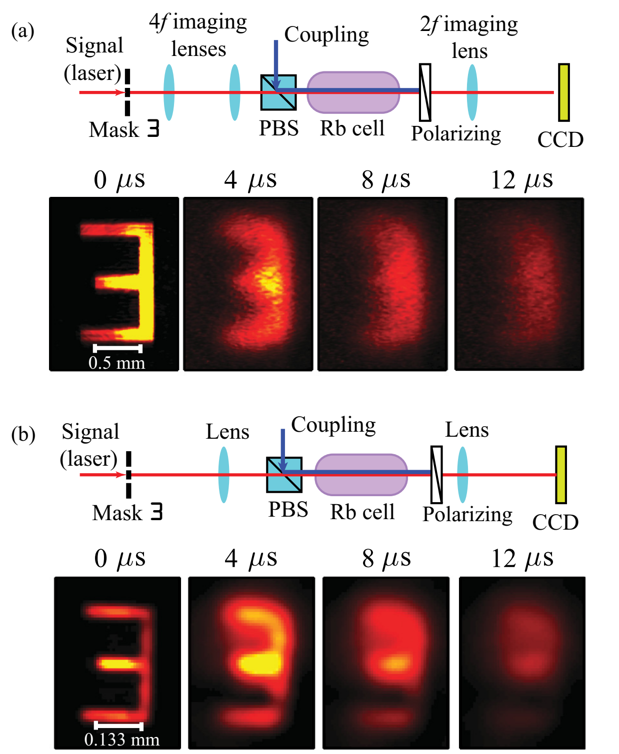

FIG. 4. (Color online) Storing two-dimensional optical images in atomic vapor. Optical images are formed with a coherent laser pulse. (a) The image plane of the mask is stored and is retrieved. (b) The Fourier transform of the mask is stored and is retrieved.

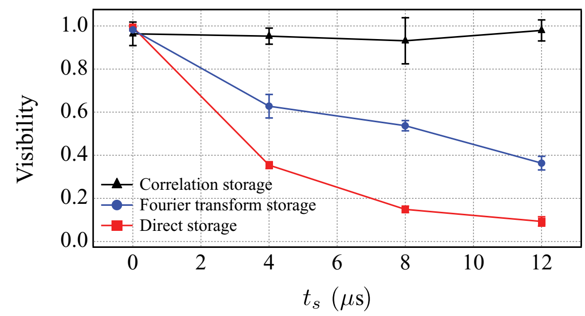

FIG. 5. (Color online) The image visibility as a function of storage duration. The direct image storage is affected very strongly by the atomic diffusion. The Fourier-transform storage works slightly better, but there are inherent limitations, which are reflected as the significant loss of image quality. The correlation storage offers nearly diffusion-free image storage—the visibility remains at unity for all storage durations.

image storage, a two-dimensional image of the same mask is imprinted on a horizontally polarized 10-μs rectangular laser pulse locked to the ^{87}Rb D_1 line $|F=1\rangle \rightarrow |F'=2\rangle$. The coupling laser, which is orthogonally polarized to the image-carrying laser beam is locked to $|F=2\rangle \rightarrow |F'=2\rangle$. The experimental data shown in Fig. 4(a) clearly demonstrate that the retrieved image quickly diffuses out and loses the image quality for longer storage duration, which is due to atomic diffusion.

It is clearly seen, by comparing Figs. 3 and 4(a), that our scheme allows diffusion-free storage of optical images in atomic vapor, which is not possible with direct image storage. This is simply due to the use of a bucket detector. Whereas, the atomic diffusion makes the retrieved images diffuse in the direct image storage, in the correlation storage, the bucket detector washes out the effect of atomic diffusion by integrating the retrieved signal. To now examine whether our approach would fare better than the Fourier-transform storage technique [13,14], an additional experiment was performed using the same vapor cell. As shown in Fig. 4(b), to put the Fourier transform (i.e., the diffraction pattern) of the mask at the center of the vapor cell, the center of the vapor cell was placed in the transform plane of a $4f$ imaging system. The $4f$ imaging system consists of two lenses ($f = 750$ mm and $f = 20$ mm) and has a magnification factor of 0.267. The experimental data are shown in Fig. 4(b). For the Fourier-transform storage, the spatial destructive interference of the dark-state polariton keeps the dark spots (zero crossings of complex amplitudes) of the Fourier-transformed image dark even with atomic diffusion, similar to topological stability of stored optical vortices [11]. Theoretically, for Fourier-transform storage, the outlines of retrieved images should remain relatively sharp while the amplitude at the outer region of the retrieved images decay much faster than that of the central region [14]. The experimental results shown in Fig. 4(b), however, demonstrate that the edges of the images also get blurred, although not as much as in Fig. 4(a). This is because, in reality, the vapor cell must be long enough to obtain a sufficient optical depth for storage. Also, the Fourier-transform storage works well only for a simple binary object [14].

To compare the image quality as a function of the storage duration for the three schemes discussed in this paper, a vertical cross section at the center of each image is taken out, and the image visibility versus the storage duration is calculated, see Fig. 5. For the direct image storage in hot atomic vapor shown in Fig. 4(a), a significant loss in the image quality is observed. The Fourier-transform storage, reported in Fig. 4(b), preserves the image quality a bit better, but the inherent limitations of the Fourier-transform storage is clearly seen with the significant loss of the image quality. On the other hand, the correlation storage approach demonstrated in Fig. 3 preserves the image quality quite faithfully even with a relatively long storage duration. (We note that the overall brightness of retrieved images is reduced due to the reduced retrieval efficiency with long storage duration, but the brightness can be increased by taking more numbers of measurement N.) In fact, the retrieved image is practically diffusion free, exhibiting nearly unity image visibilities for all the storage durations tested in this paper. Clearly, atomic diffusion does not affect the quality of the image stored using the correlation image storage approach.

One of the advantages of the correlation imaging storage technique over the optical phase-shift lithography and the Fourier-transform storage is that the optical image is formed with incoherent light. The optical phase-shift lithography and the Fourier-transform storage rely on spatial coherence of the dark-state polariton, which requires that the optical image is formed with coherent light. Since the vast majority of imaging applications uses incoherent light for imaging, our approach demonstrated in this paper could have practical implications in all-optical image storage.

Another interesting aspect we wish to mention is that, although incoherent light is used for correlation imaging storage, the correlation imaging (or ghost imaging) makes use of the second-order coherence of the light field [18,22]. Thus, the correlation imaging technique can image not only a pure phase object [23,24], but also a complex grayscale object [25]. This suggests that it should be possible to envision all-optical storage of complex phase and amplitude information of an object using warm (hot) atomic vapor and the correlation imaging technique discussed in this paper.

To summarize, we have demonstrated diffusion-free image storage in warm atomic vapor using the correlation imaging technique. Since the correlation imaging is inherently diffusion free, the atomic diffusion and the storage duration do not affect the image quality. Furthermore, this scheme allows all-optical storage of images formed with incoherent light.

This work was supported in part by the National Research Foundation of Korea (Grants No. 2009-0084473, No. 2011-0021452, and No. 2012-002588). Y.-W.C. acknowledges support from the National Junior Research Fellowship (Grant No. 2011-0010895).

[1] L. V. Hau, S. E. Harris, Z. Dutton, and C. Behroozi, Nature (London) **397**, 594 (1999).
[2] M. M. Kash, V. A. Sautenkov, A. S. Zibrov, L. Hollberg, G. R. Welch, M. D. Lukin, Y. Rostovtsev, E. S. Fry, and M. O. Scully, Phys. Rev. Lett. **82**, 5229 (1999).
[3] D. F. Phillips, A. Fleischhauer, A. Mair, R. L. Walsworth, and M. D. Lukin, Phys. Rev. Lett. **86**, 783 (2001).
[4] Kocharovskaya, Y. V. Rostovtsev, and M. O. Scully, Phys. Rev. Lett. **86**, 628 (2001).
[5] J. B. Khurgin, Adv. Opt. Photon. **2**, 287 (2010).
[6] R. S. Tucker, J. Lightwave Technol. **23**, 4046 (2005).
[7] A. I. Lvovsky, B. C. Sanders, and W. Tittel, Nat. Photonics **3**, 706 (2009).
[8] R. M. Camacho, C. J. Broadbent, I. Ali-Khan, and J. C. Howell, Phys. Rev. Lett. **98**, 043902 (2007).
[9] M. Tomita, P. Sultana, A. Takami, and T. Matsumoto, Opt. Express **18**, 12599 (2010).
[10] P. Sultana, A. Takami, T. Matsumoto, and M. Tomita, Opt. Lett. **35**, 3414 (2010).
[11] R. Pugatch, M. Shuker, O. Firstenberg, A. Ron, and N. Davidson, Phys. Rev. Lett. **98**, 203601 (2007).
[12] M. Shuker, O. Firstenberg, R. Pugatch, A. Ron, and N. Davidson, Phys. Rev. Lett. **100**, 223601 (2008).
[13] P. K. Vudyasetu, R. M. Camacho, and J. C. Howell, Phys. Rev. Lett. **100**, 123903 (2008).
[14] L. Zhao, T. Wang, Y. Xiao, and S. F. Yelin, Phys. Rev. A **77**, 041802(R) (2008).
[15] G. Heinze, A. Rudolf, F. Beil, and T. Halfmann, Phys. Rev. A **81**, 011401(R) (2010).
[16] M. Fleischhauer and M. D. Lukin, Phys. Rev. Lett. **84**, 5094 (2000).
[17] F. Ferri, D. Magatti, A. Gatti, M. Bache, E. Brambilla, and L. A. Lugiato, Phys. Rev. Lett. **94**, 183602 (2005).
[18] G. Scarcelli, V. Berardi, and Y. Shih, Phys. Rev. Lett. **96**, 063602 (2006).
[19] Y.-W. Cho, J.-E. Oh, and Y.-H. Kim, Opt. Express **20**, 5809 (2012).
[20] W. Gong and S. Han, Opt. Lett. **36**, 394 (2011).
[21] Y.-W. Cho and Y.-H. Kim, Phys. Rev. A **82**, 033830 (2010).
[22] M. D'Angelo, Y.-H. Kim, S. P. Kulik, and Y. Shih, Phys. Rev. Lett. **92**, 233601 (2004).
[23] M. Bache, D. Magatti, F. Ferri, A. Gatti, E. Brambilla, and L. A. Lugiato, Phys. Rev. A **73**, 053802 (2006).
[24] T. Shirai, T. Setälä, and A. T. Friberg, Phys. Rev. A **84**, 041801(R) (2011).
[25] F. Ferri, D. Magatti, L. A. Lugiato, and A. Gatti, Phys. Rev. Lett. **104**, 253603 (2010).